Carbohydrate Polymers 80 (2010) 145–153

Contents lists available at ScienceDirect

Carbohydrate Polymers

journal homepage: www.elsevier.com/locate/carbpol

Starch nano-biocomposites based on needle-like sepiolite clays

Frédéric Chivrac [a], Eric Pollet [a], Marc Schmutz [b], Luc Avérous [a,*]

[a] LIPHT-ECPM, Université de Strasbourg, 25 rue Becquerel, 67087 Strasbourg Cedex 2, France
[b] ICS, UPR 22, Université de Strasbourg, 23 rue Becquerel, 67034 Strasbourg Cedex, France

ARTICLE INFO

Article history:
Received 6 July 2009
Received in revised form 27 October 2009
Accepted 5 November 2009
Available online 15 November 2009

Keywords:
Nanocomposites
Plasticized starch
Sepiolite

ABSTRACT

This paper reports the successful elaboration and study of plasticized starch nano-biocomposites elaborated with needle-shaped nanofillers, namely natural sepiolite (SEP-Na) and sepiolite organo-modified with cationic starch (OSEP-CS). The transmission electronic microscopy has highlighted a well-nanodispersed morphology with almost individual sepiolite needles. It has been shown that different micro/nano-structurations are obtained with the variation of the cationic starch content. Depending on its concentration, it could act as a flocculating agent or a compatibilizer. Finally, uniaxial tensile tests have evidenced the interest in using sepiolite nanofillers to tune the plasticized starch properties, even in comparison with the more common montmorillonite-based nano-biocomposites. Thanks to these needle-shaped nanofillers, the material stiffness is increased without decreasing its properties at break.

1. Introduction

The new sustainable development policies, combined with the increasing environmental concern, imply the development of environmentally friendly materials. Several authors have already demonstrated the possibility to transform native starch granules into thermoplastic-like materials under destructuring and plasticizing conditions (Swanson, Shogren, Fanta, & Imam, 1993; Tomka, 1991). However, the mechanical properties of this promising material have to be enhanced to compete with conventional petroleum-based polymers (Averous, 2004).

Nanofiller (nano-sized filler) incorporation into bio-based matrices, to produce nano-biocomposite materials, could be a powerful solution to improve these properties, even at low nanofillers content (typically less than 5 wt.%) (Alexandre & Dubois, 2000; Bordes, Pollet, & Averous, 2009; Sinha Ray & Okamoto, 2003). Compared to conventional composites, the main reason for such improvement relies on the large interface area resulting in high interactions between the polymer matrix and the nanofillers (Alexandre & Dubois, 2000; Bordes et al., 2009; Dennis et al., 2001; Sinha Ray & Okamoto, 2003).

Up to now, the most intensive researches have been focused on layered silicates, and especially on montmorillonites, as the reinforcing phase. However, these nanofillers are not the only type of nanoclay that can be incorporated into polymer matrices. Recently, some studies have been focused on the use of sepiolite, a nanofiller with a needle-like structure, to elaborate nanocomposites (Bhattacharya, Maiti, & Bhowmick, 2009; Bilotti, Fischer, & Peijs, 2008; Bilotti et al., 2009; Bokobza, Burr, Perrin, & Pagnotta, 2004; Chen, Zheng, Sun, & Jia, 2007; Darder et al., 2006; Duquesne, Moins, Alexandre, & Dubois, 2007; Fernandes, Ruiz, Darder, Aranda, & Ruiz-Hitzky, 2009; Garcia, Hoyos, Guzman, & Tiemblo, 2009; Ma, Bilotti, Peijs, & Darr, 2007a; Xie et al., 2007; Zheng, 2006). This nanofiller is a microcrystalline hydrated magnesium silicate of theoretical unit cell formula $Mg_8Si_{12}O_{30}(OH)_4 \cdot (H_2O)_4 \cdot 8H_2O$. It shows an alternation of blocks and channels that grow up in the fiber direction. The blocks are basically constituted by two layers of tetrahedral silica sandwiching a central octahedral magnesium oxide–hydroxide layer (Fig. 1). Some isomorphic substitutions occur inside these central layers creating a negative charge naturally counterbalanced by the presence of inorganic cations (Na^+, Ca^{2+}...). The sepiolite channels are filled both with the coordinated water molecules, which are bonded to the Mg^{2+} ions located at the edges of octahedral sheets, and with the zeolithic water, which is associated to the structure by hydrogen bonding. The discontinuity of the silica sheets gives rise to the presence of silanol groups (Si–OH) at the edges of the external surface of the sepiolite nanoparticles.

Thus, the first aim of this study was the elaboration of starch-based nano-biocomposites with the use of sodium sepiolite (SEP-Na) nanofillers. Moreover, since we have recently demonstrated that the adsorption of cationic starch at the montmorillonite surface favors the exfoliation process into plasticized starch matrix (Chivrac, Pollet, Schmutz, & Averous, 2008b), sepiolite organo-modified with cationic starch (OSEP-CS) has been prepared and then incorporated into the plasticized starch matrix. Special atten-

* Corresponding author. Tel.: +33 3 68 852 707; fax: +33 3 68 852 716.
E-mail address: luc.averous@unistra.fr (L. Avérous).

0144-8617/$ - see front matter © 2009 Elsevier Ltd. All rights reserved.
doi:10.1016/j.carbpol.2009.11.004

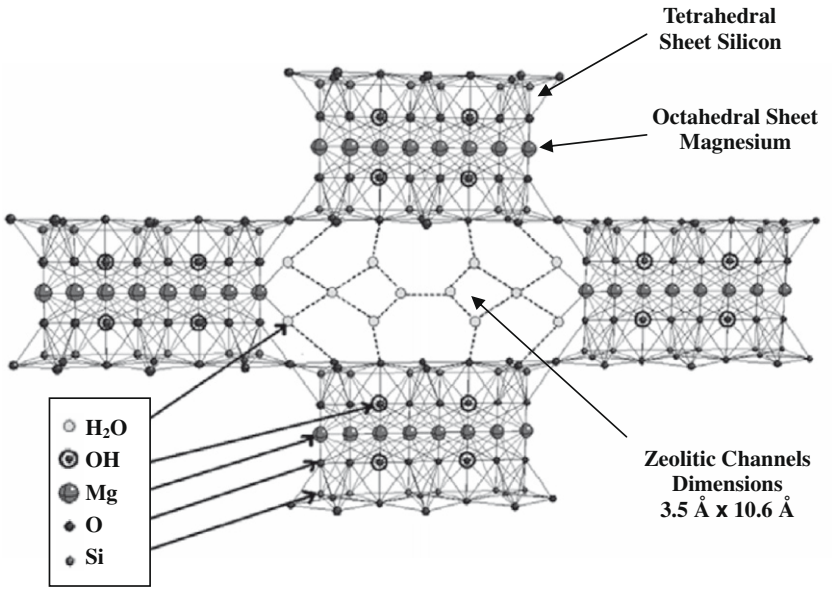

Fig. 1. Sepiolite structure-projection onto the (001) plane.

tion has been paid to describe and understand the relationship between the nanofiller structuration into the matrix and the resulting properties. Finally, the mechanical properties of the starch/sepiolite nano-biocomposites have been compared to those previously reported for starch nano-biocomposites based on montmorillonite lamellar clay and on cellulose whiskers nanofibers to highlight the great potential of the sepiolite nanoclay.

2. Experimental

2.1. Materials

Wheat starch (WS) was supplied by Roquette (France). The amylose and amylopectin contents are 23% and 77%, respectively. Residual protein content is less than 1%. The glycerol used as non-volatile plasticizer was supplied by the Société Française des Savons (France) and is a 99.5% purity product. The cationic starch has been supplied by Roquette (France). Its charge density is 944 μequiv g^{-1}. The cationic functions are quaternary ammonium with chloride as counter-anion. The Pangel® S9 sodium sepiolite (SEP-Na) was supplied by Tolsa (Spain) and has a cationic exchange capacity (CEC) of 150 μequiv g^{-1}. The Dellite® LVF sodium montmorillonite (MMT-Na) was supplied by Laviosa Chimica Mineraria S.p.A. (Italy) and has a cationic exchange capacity (CEC) of 1050 μequiv g^{-1}.

2.2. Samples preparation

2.2.1. Organo-modified sepiolite preparation

The sodium sepiolite organo-modification was carried out with cationic starch by dispersion/adsorption technique. An oversimplified representation of this organo-modification protocol is represented in Fig. 2. Four different types of organo-modified sepiolite, OSEP-1CS, OSEP-2CS, OSEP-4CS and OSEP-6CS corresponding, respectively, to one, two, four and six charge equivalence between the sepiolite and the cationic starch, have been prepared. First, 5 g of SEP-Na was introduced into 250 mL of distilled water and dispersed in an ultra-sonic bath at 60 °C for 4 h. In parallel, from 0.79 to 4.77 g of cationic starch (depending on the cationic starch content desired) were introduced in 30 mL of distilled water and solubilized in an ultra-sonic bath at 60 °C for 1 h. Then, the two solutions were pooled together and placed for 1 day at 60 °C in an ultra-sonic bath. The solution was filtered and washed with 1 L of distilled water at 60 °C to remove the formed salt (NaCl) during the cationic starch adsorption. Then, the filtrate was lyophilized to obtain a dry powder of sepiolite organo-modified with cationic starch (OSEP-CS) that will be further incorporated into the plasticized starch matrix.

2.2.2. Organo-modified montmorillonite preparation

The MMT-Na organo-modification has been carried out with cationic starch by exfoliation/adsorption technique. MMT-Na (5 g) is introduced in 250 ml of distilled water and dispersed in ultra-sonic bath at 60 °C for 4 h. In parallel, 5.6 g of cationic starch is introduced in 250 ml of distilled water and solubilized in ultra-sonic bath at 60 °C for 1 h. These proportions correspond to the charge equivalence between MMT and cationic starch. Then, the two solutions are pooled together and placed for 1 day at 60 °C in ultra-sonic bath. The solution is filtered and washed with 1 L of distilled water at 60 °C to remove the formed salt (NaCl) during the cationic starch adsorption. Then, the filtrate is lyophilized to obtain the cationic starch organo-modified montmorillonite (OMMT-CS).

2.2.3. Starch dry-blends preparation

The formulation used in this study contained 54 wt.% of native starch, 23 wt.% of glycerol and 23 wt.% of water. Native wheat starch granules were first dried overnight at 70 °C in a ventilated oven to remove the free water (~10 wt.% of the materials depending on the relative atmosphere humidity and temperature). Then, the starch powder was introduced into a turbo-mixer and the glycerol was slowly added under stirring. After complete addition of glycerol, the mixture was mixed at high speed (1700 rpm) to obtain a homogeneous dispersion. The mixture was then placed in a ventilated oven at 170 °C for 40 min and occasionally stirred, allowing vaporization of the bound water and diffusion of the glycerol into the starch granules. Such dry-blend protocol allows the preparation of plasticized starch with high glycerol content without exudation phenomenon, mainly thanks to the stronger interactions established between the polysaccharide chains and the glycerol plasticizer (Averous, Fringant, & Moro, 2001). Then, to obtain the adequate moisture content, a determined quantity of

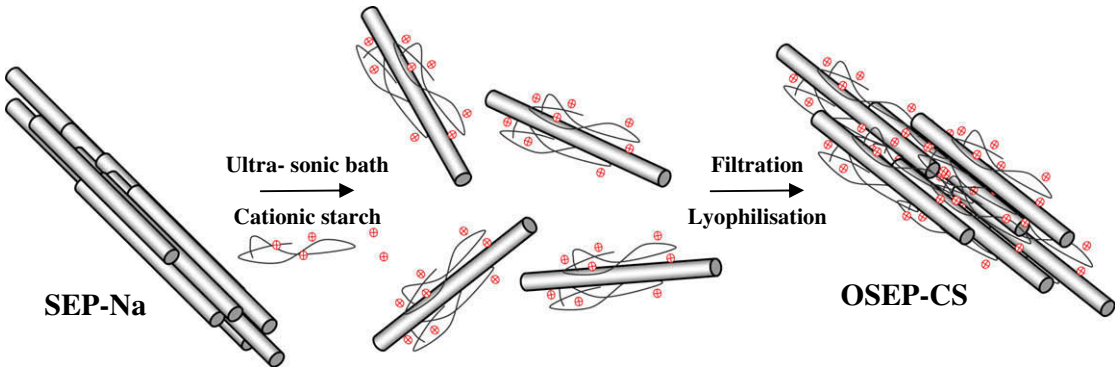

Fig. 2. Oversimplified representation of the SEP-Na organo-modification by dispersion/adsorption technique.

water is added to this dry-blend after cooling and mixed at high speed (1700 rpm). The dry-blend (powder) was then stored in polyethylene bag.

2.2.4. Nano-biocomposites elaboration

To obtain nano-biocomposites, 3 and 6 wt.% of nanoclay inorganic matter compared to the weight of starch and glycerol (1.38 and 2.86 g of clay inorganic fraction, respectively) have been added into the dry-blend. This mixture has been processed by mechanical kneading with a counter-rotating internal batch mixer, Rheocord 9000 (Haake, USA), at 70 °C for 20 min with a rotor speed of 150 rpm. After melt processing, molded specimens and films were obtained by hot-pressing at 110 °C applying 20 MPa pressure for 15 min. The nano-biocomposite samples were then allowed to equilibrate at 57% RH (relative humidity percentage) for 1 month in a controlled humidity chamber before characterization. Throughout this paper, the samples are designated WS/XXX *y*% where XXX stands for the type of (organo)clay and *y* for the weight percentage of clay inorganic fraction.

2.3. Characterization

2.3.1. TEM characterization

For transmission electronic microscopy (TEM) observation, the samples were microtomed at low temperature (−80 °C) using a Diatome AG-microtome (Switzerland) equipped with a diamond knife. The ultra thin sections (nominal thickness 60 nm) were examined using a Philips CM 12 (Netherlands) transmission electron microscope using an acceleration voltage of 120 kV.

2.3.2. XRD characterization

The X-ray diffraction (XRD) morphological analyses were performed on a powder diffractometer Siemens D5000 (Germany) using Cu (Kα) radiation (λ = 1.5406 Å) at room temperature in the range of 2θ = 3–40° by step of 0.01° of 4 s each.

2.3.3. TGA characterization

The thermogravimetric analyses (TGA) were performed on a SDT Q600 apparatus from TA Instruments (USA). For all starch/sepiolite nano-biocomposites, the analyses were carried out under "synthetic air" which is a mixture of 75% N_2 and 25% O_2. The samples (ca. 10 mg placed in a platinum pan) were heated from 20 to 600 °C at 10 °C/min.The clay content in inorganics (in wt.%) of each composite was assessed by the combustion residue left at 600 °C. The degradation temperature was determined from the peak temperature of the derivative weight loss curve.

2.3.4. Mechanical tests

Uniaxial tensile tests were carried out with an Instron tensile testing machine (model 4204, USA), on dumbbell-shaped specimens; at 25 °C with a constant deformation rate of 5 mm/min. For each formulation five samples were tested.

3. Results and discussion

3.1. Morphological characterization of the starch nano-biocomposites

Fig. 3 displays the optical microscopy micrographs obtained from WS/SEP-Na, WS/OSEP-1CS, WS/OSEP-2CS and WS/OSEP-4CS 6 wt.%. From these observations, it is seen that no aggregates are observed for WS/SEP-Na nano-biocomposites (Fig. 3a). Surprisingly, large clay aggregates with a mean diameter around 200–300 μm are observed when the nanofiller is organo-modified with one equivalent of cationic starch (Fig. 3b). This result is unexpected since cationic starch is assumed to act as a compatibilizer. To explain these sepiolite aggregates, one may suppose that, for OSEP-1CS, cationic starch strongly interacts with sepiolite surface and establishes "bridges" between the nanofiller needles leading to flocculated structure. This assumption is supported by the low CEC of the sepiolite, which leads to a low charge density. Thus, when a cationic starch is adsorbed on the sepiolite surface, the probability for this polycation to be adsorbed on another sepiolite needle (to compensate its excess of positive charge) is not negligible and may lead to the formation of aggregates. On the opposite, as seen on the optical microscopy micrographs presented in Figs. 3c and d, no more aggregates are observed for nano-biocomposites elaborated with OSEP-2CS and OSEP-4CS. This behavior is likely due to the higher extent of electrostatic repulsions and steric hindrance resulting from the higher content in macromolecular polycations.

To better observe the nanofillers structuration, TEM characterization has been performed on these materials. Figs. 4 and 5 show typical TEM micrographs of WS/SEP-Na 3 wt.% and WS/OSEP-4CS 3 wt.%, respectively. At low magnification (Figs. 4a and 5a), a heterogeneous morphology is observed with domains rich in sepiolite nanofiller and some regions without clay. This heterogeneity has been previously reported with plasticized starch/montmorillonite nano-biocomposites (Chivrac et al., 2008b). It is linked to the high glycerol content of the plasticized starch formulation, which is known to induce a phase separation between domains with high and low glycerol content (Averous, 2004). In the domains rich in sepiolite, the TEM micrographs at high magnification (Figs. 4b and 5b) show limited amounts of very small clay aggregates and a large proportion of almost individually and randomly dispersed needles for both WS/SEP-Na and WS/OSEP-4CS. On one hand, for the sodium sepiolite, this result seems to indicate that the silanol

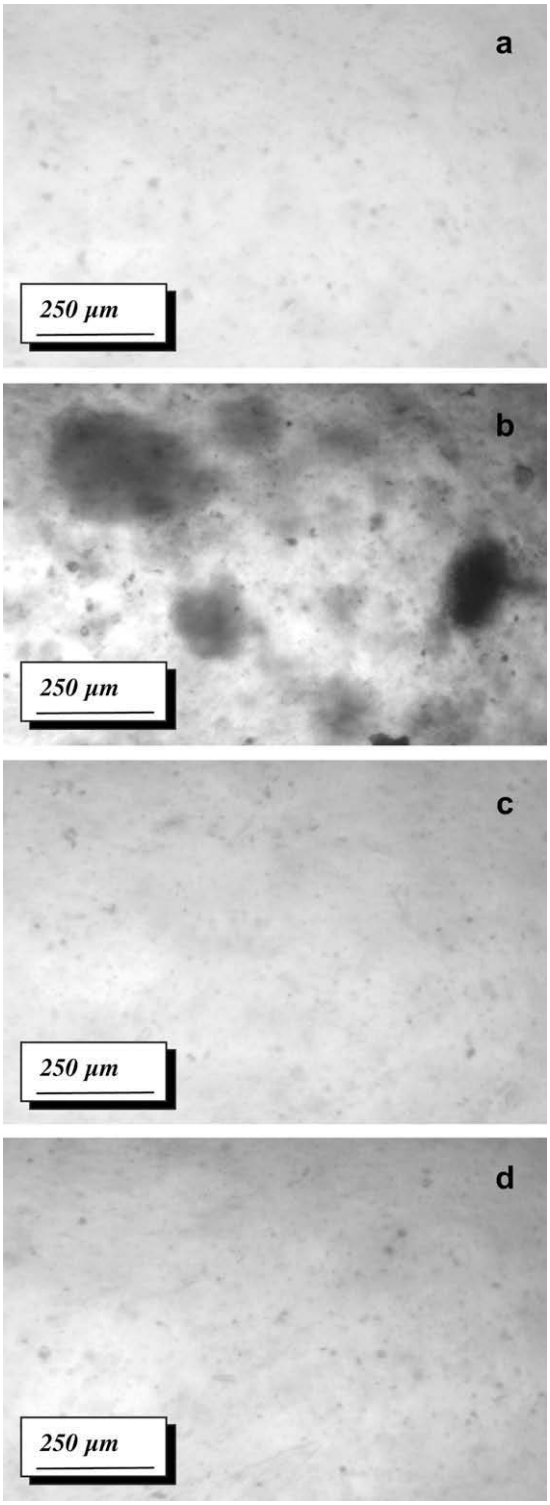

Fig. 3. Optical microscopy micrographs of (a) WS/SEP-Na 6 wt.%, (b) WS/OSEP-1CS 6 wt.%, (c) WS/OSEP-2CS 6 wt.% and (d) WS/OSEP-4CS 6 wt.%.

groups of the needles and the hydroxyl groups of the starch chains could interact together with the formation of hydrogen bonds, which facilitate the nanofiller dispersion. On the other hand, for the organo-modified sepiolite, even if the OSEP-1CS leads to a highly aggregated structure, a good and effective nano-dispersion of the organo-modified sepiolite needles is achieved with cationic starch content higher than one CEC. Such behavior could be explained by the excess of positive charge which may generate nanoparticles repulsion. These electrostatic repulsions together with some steric hindrance issues that cannot be excluded make impossible, or at least very limited, the sepiolite needles aggregation. Thus, for higher concentration than one sepiolite CEC, cationic starch fully acts as a compatibilizer.

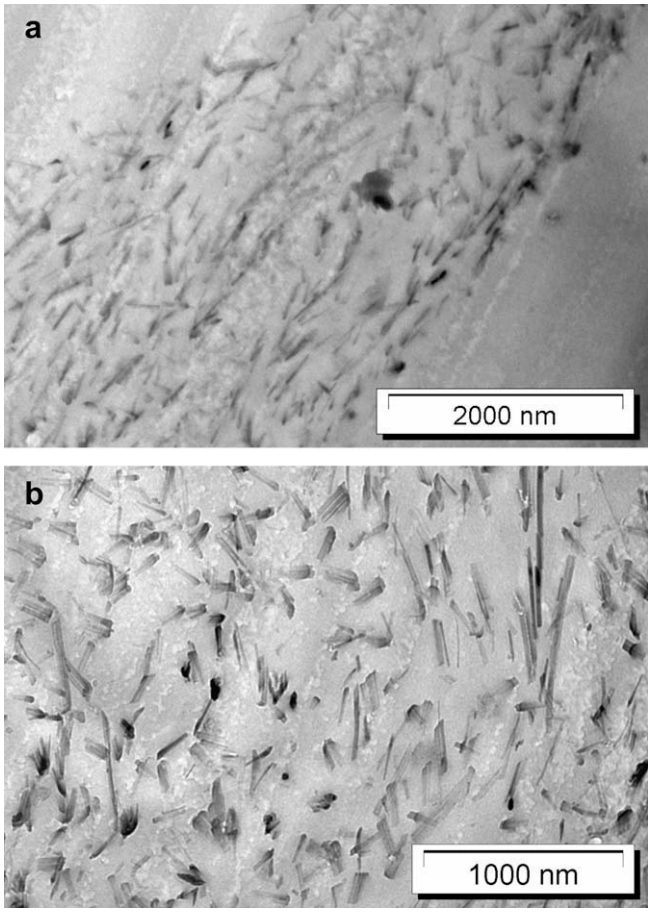

Fig. 4. TEM pictures of WS/SEP-Na 3 wt.% nano-biocomposites at (a) low magnification and (b) high magnification level.

Fig. 6 displays the typical X-ray diffraction (XRD) curves recorded for SEP-Na, WS, WS/SEP-Na 6 wt.%, WS/OSEP-1CS 6 wt.% and WS/OSEP-4CS 6 wt.%. The diffractogram of the SEP-Na displays an intense peak at 7.5° corresponding to the internal channel reflections of the needle structure (Darder et al., 2006). The other diffraction peaks correspond to the sepiolite crystal structure. As expected, after dispersion in the starch matrix, the sepiolite internal channel diffraction peak is not shifted, attesting that the channel structure of the primary particles remains unchanged. On the contrary, the XRD analyses performed on starch/montmorillonite nano-biocomposites, that have been previously described elsewhere (Chivrac et al., 2008b), showed different shifts in the clay diffraction peak. For the sake of clarity, these results will be simply summarized hereafter. On one hand, the diffraction patterns of WS/MMT-Na nano-biocomposites display a peak at 4.9° corresponding to a basal spacing value (d_{001}) of 18 Å. This d_{001} is already well reported in the literature and is commonly attributed to the glycerol intercalation (Chivrac, Pollet, & Averous, 2009; Cyras, Manfredi, Ton-That, & Vazquez, 2008; Dean, Yu, & Wu, 2007; Ma, Yu, & Wang, 2007b; Pandey & Singh, 2005; Park, Lee, Park, Cho, & Ha, 2003; Park et al., 2002). Thus, the presence of this diffraction peak means that these materials are mainly nanocomposites with low intercalation extent of the starch chains and preferential

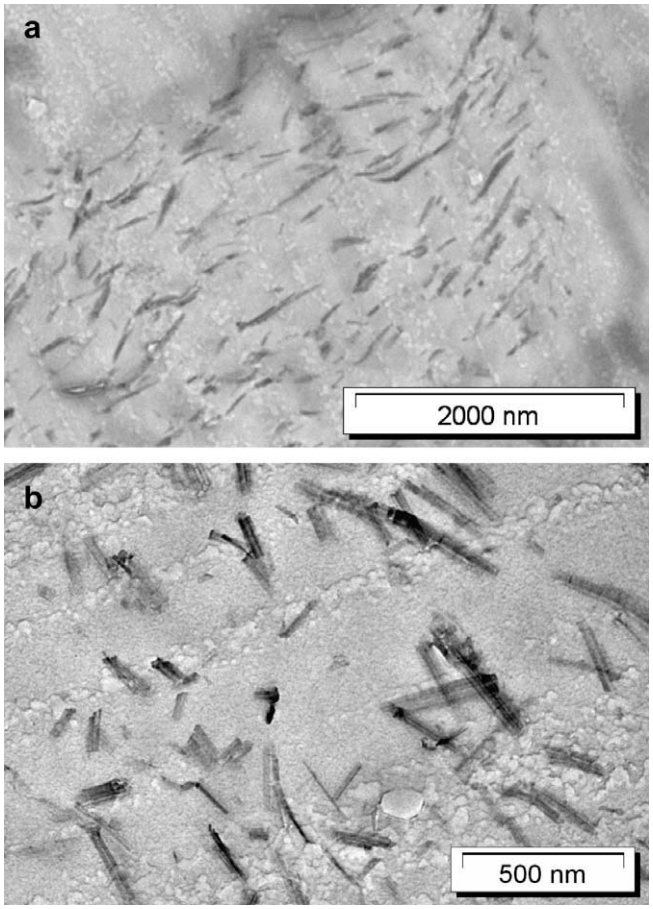

Fig. 5. TEM pictures of WS/OSEP-4CS 3 wt% nano-biocomposites at (a) low magnification and (b) high magnification level.

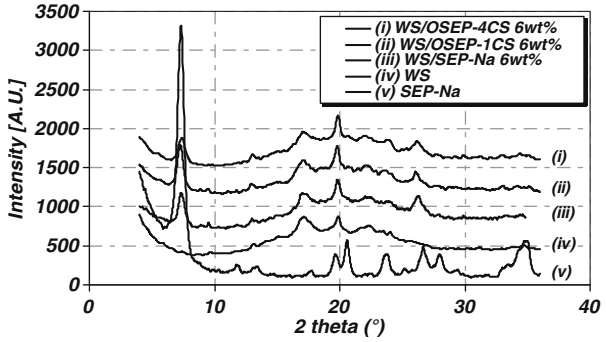

Fig. 6. XRD patterns for SEP-Na, WS, WS/SEP-Na and WS/OSEP-CS nano-biocomposites.

glycerol intercalation. On the other hand, the diffraction patterns of WS/OMMT-CS nano-biocomposites display no diffraction peak attesting for a good nano-dispersion of the OMMT-CS with a high extent of exfoliation in the starch matrix.

Besides, it can be seen from Fig. 6 that the diffractogram obtained for the neat matrix displays E_H-Type crystallization peak at $2\theta = 17.2°$, corresponding to the amylopectine recrystallization. V_H-type crystallization peaks are also observed at $2\theta = 19.9°$ and 22.5° and correspond to the process induced amylose crystallization into single helical structure (Van Soest, Hulleman, De Wit, & Vliegenthart, 1996). No significant evolution of these E_H-Type and V_H-Type crystallization peaks are observed for the starch/sepiolite nano-biocomposites samples. However, their diffractograms display a new diffraction peak located at 26.4°, corresponding to a crystal lattice structure of 3.4 Å (calculated from the Bragg's law). Such a new diffraction peak has already been reported into starch/tunicin whiskers composites. It is attributed to amylopectine crystallization at the filler interface and is favored by hydrogen bonds established between the filler and the macromolecules (Neus Angles & Dufresne, 2000). Thus, these results suggest the occurrence of a new crystal structure likely induced by the interactions established between the numerous silanol groups located at the edge of the sepiolite needles and the hydroxyl groups of the polysaccharide chains. Such behavior of sepiolite inducing or promoting a specific type of crystallinity at the polymer/clay interface as already been reported in the case of PP/sepiolite nanocomposites (Bilotti et al., 2008; Ma et al., 2007a) and for PA6/sepiolite nanocomposites (Bilotti et al., 2009). Interestingly, the XRD analyses performed on starch/montmorillonite nano-biocomposites (Chivrac et al., 2008b) did not show such filler induced new type of crystallization.

3.2. Thermal stability

The thermal stability of the plasticized starch-based nano-biocomposites has been assessed by thermogravimetric analysis (TGA). Fig. 7a displays part of the typical thermogram obtained for pristine plasticized wheat starch, three different steps of weight loss being detected at 292, 318 and 526 °C (the latter is not shown here). The first step corresponds to the glycerol plasticizer volatilization. Indeed, this weight loss matches the glycerol content of the formulation and it is not observed for non-plasticized starch matrix (not displayed here). The two others weight losses correspond to the starch amylose and amylopectin thermal degradation.

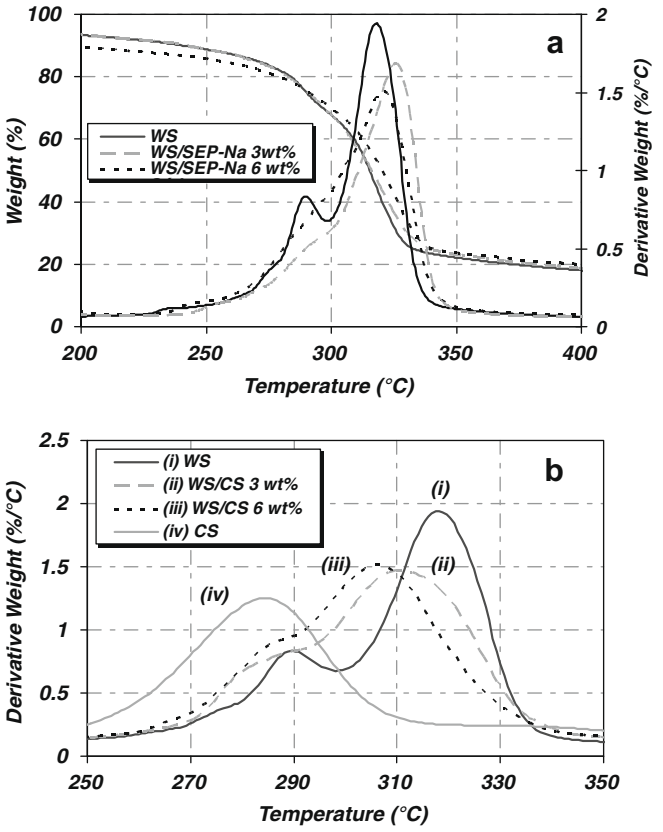

Fig. 7. (a) TG and DTG curves recorded for WS, WS/SEP-Na 3 wt.% and 6 wt.%. (b) DTG curves recorded for WS, WS/CS 3 wt.%, WS/CS 6 wt.% and CS (cationic starch).

Fig. 7a also presents the thermograms of the plasticized wheat starch nano-biocomposites filled with 3 and 6 wt.% of SEP-Na. Regarding the derivative weight loss curves (DTG), the starch maximum degradation temperature, observed at 318 °C in the neat matrix, is shifted towards higher temperatures (321 and 326 °C for a SEP-Na content of 3 and 6 wt.%, respectively) and is correlated with the SEP-Na content. This increase in the degradation temperature is commonly observed in montmorillonite-based nanocomposites. It is mainly attributed to an increase in the tortuosity of the diffusion pathway induced by the clay dispersion, which limits the diffusion of the pyrolysis gases to the material surface (Alexandre & Dubois, 2000; Sinha Ray & Okamoto, 2003). According to the needle-like structure of the SEP-Na, an increase in the tortuosity of the diffusion pathway is less plausible, thus the delayed and limited diffusion of gases is more likely related to extensive molecular interactions (physi- and/or chemi-sorption) occurring at the sepiolite/matrix interphase. Such behavior has been reported for PU/sepiolite nanocomposites (Chen et al., 2007) and assigned to the strong interactions leading to a physical network enhancing the PU thermal stability. Increased thermal stability in presence of sepiolite has also been observed for PE (Garcia et al., 2009) and mainly explained by the ability of sepiolite to form a protective inorganic layer at the surface of the degrading material, this layer being thicker than the one obtained for montmorillonite. Both the strong interactions and the protective layer formation could explain the slight increase in thermal stability observed for the WS/SEP-Na nano-biocomposites.

Fig. 8 displays the thermograms recorded for the pristine plasticized wheat starch matrix and the nano-biocomposites filled with 6 wt.% of OSEP-1CS, OSEP-2CS, OSEP-4CS and OSEP-6CS. Contrary to the SEP-Na nano-biocomposites, a decrease in the starch maximum degradation temperature (319, 316, 312 and 309 °C, respectively) is observed. This decrease is correlated with the cationic starch content (1, 2, 4 and 6 CS equivalent, respectively). A similar trend is observed for montmorillonite-based materials with starch maximum degradation temperatures of 312 and 308 °C for OMMT-CS contents of 3 and 6 wt.%, respectively (not shown here). To highlight the cationic starch influence, blends of plasticized starch and cationic starch have been elaborated with a ratio of 97 wt.%/3 wt.% and 94 wt.%/6 wt.% and then have been analyzed by TGA (Fig. 7b). A clear dependence between the cationic starch content and the degradation temperature of the blend is observed, the blends elaborated with 3 and 6 wt.% of cationic starch presenting a maximum degradation temperature located at 311 and 306 °C, respectively. In addition, pure cationic starch has also been studied, its main degradation being observed at 284 °C. The comparison of the calculated TGA of a polymer mixture with the linear combination of weight loss curves of components can reveal whether interactions between mixture components occur on thermal degradation of the mixture. For the plasticized starch/cationic starch systems, the calculated and the experimental curves are not superimposed, the experimental curve displaying a lower degradation temperature than the calculated one (not shown here). Thus, one may suppose, that the by-products generated during the cationic starch degradation favor the plasticized starch thermal degradation. Further experiments have to be carried out to better understand this degradation reaction mechanism.

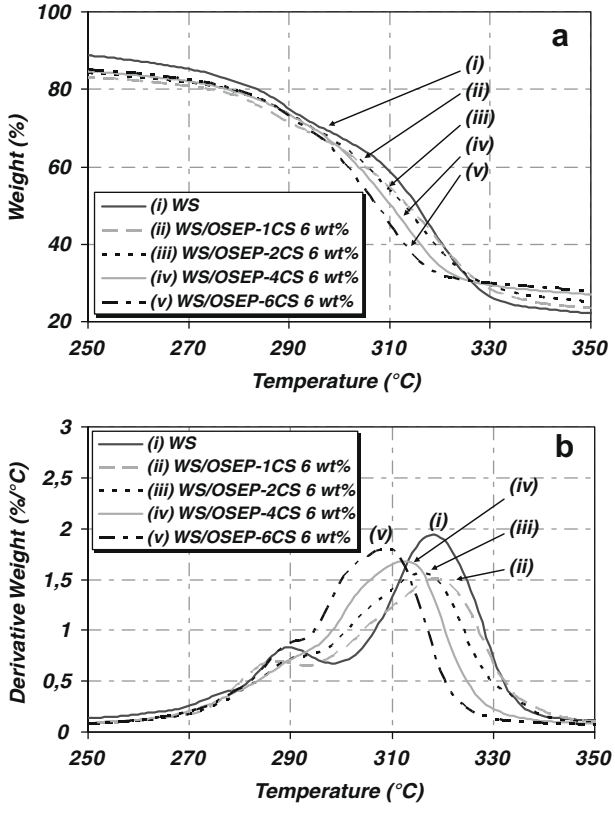

Fig. 8. (a) TG and (b) DTG curves recorded for WS, WS/OSEP-1CS 6 wt.%, WS/OSEP-2CS 6 wt.%, WS/OSEP-4CS 6 wt.% and WS/OSEP-6CS 6 wt.%.

3.3. Mechanical properties

Table 1 reports the mechanical properties (Young modulus, strain and stress at break) of the raw starch matrix, of the starch blends elaborated with 3 and 6 wt.% of cationic starch and of the nano-biocomposites filled with both sepiolite and montmorillonite organo-modified or not. Compared to the pristine matrix, no significant variations are observed in the mechanical properties of the starch/cationic starch blends. Thus, we can conclude that the cationic starch content used to organo-modify the nanofillers does not influence the nano-biocomposites mechanical properties.

For all the nano-biocomposites, an increase in the matrix stiffness is obtained with clay incorporation. This stiffness increase is commonly observed in nanocomposite systems and is related to the nanofiller dispersion state and more precisely on the filler surface-polymer chain segments interactions which reduce chain mobility and hence enhance macroscopic rigidity (Chivrac et al., 2008a; Luo & Daniel, 2003). In addition, the new crystalline structure induced by the sepiolite incorporation raises the overall material crystallinity and also contributes to the stiffness increase. For the WS/OSEP-CS hybrids, a relationship between the amount of cationic starch adsorbed on the sepiolite and the Young's modulus is observed, the highest modulus being obtained for the WS/OSEP-4CS samples. According to the presented results, it seems that further addition of cationic starch does not influence the final material stiffness. Moreover, the Young's modulus values are higher than those of the SEP-Na samples. Since the cationic starch alone does not influence the mechanical properties of the starch material, this behavior can be explained by the cationic starch affinity toward starch material which generates more interactions between the nanofiller and the matrix.

The mechanical properties of the nano-biocomposites filled with 3 and 6 wt.% of both MMT-Na and OMMT-CS have been presented in a previous article (Chivrac et al., 2008b). Comparing these data with those obtained from starch/sepiolite nano-biocomposites, it is clearly seen that the WS/SEP-Na and WS/OSEP-CS stiffness values are higher than those of the corresponding montmorillonite nano-biocomposites. For the non-modified nanofillers, this can be explained by the materials morphology. Indeed, even if an effective nanoscale dispersion is obtained with the sodium sepiolite, the

Table 1
Starch nano-biocomposites mechanical properties.

	Young's modulus (MPa)	Strain at break (%)	Stress at break (MPa)
WS	28.3 ± 0.9	31.7 ± 1.5	2.24 ± 0.04
WS/CS 3 wt%	27.9 ± 0.5	32.7 ± 2.0	2.26 ± 0.12
WS/CS 6 wt%	28.1 ± 1.8	32.5 ± 3.1	2.24 ± 0.11
WS/SEP-Na 3 wt.%	45.3 ± 0.7	36.5 ± 2.1	2.91 ± 0.06
WS/SEP-Na 6 wt.%	67.3 ± 2.3	31.0 ± 1.0	2.99 ± 0.04
WS/OSEP-1CS 6 wt.%	71.9 ± 8.9	27.4 ± 1.4	3.09 ± 0.18
WS/OSEP-2CS 6 wt.%	74.8 ± 4.5	32.6 ± 0.7	3.17 ± 0.09
WS/OSEP-4CS 3 wt.%	49.1 ± 1.5	36.1 ± 2.1	2.85 ± 0.12
WS/OSEP-4CS 6 wt.%	76.0 ± 1.9	35.2 ± 1.5	3.21 ± 0.13
WS/OSEP-6CS 6 wt.%	74.8 ± 2.6	34.6 ± 0.7	3.19 ± 0.09
WS/MMT-Na 3 wt.%[a]	35.6 ± 0.6	27.3 ± 0.6	2.32 ± 0.08
WS/MMT-Na 6 wt.%[a]	39.2 ± 1.4	21.0 ± 0.8	1.90 ± 0.06
WS/OMMT-CS 3 wt.%[a]	39.4 ± 0.9	32.5 ± 0.8	2.43 ± 0.06
WS/OMMT-CS 6 wt.%[a]	46.5 ± 1.2	33.3 ± 2.0	2.63 ± 0.16

[a] Results already published elsewhere (Chivrac et al., 2008a).

WS/MMT-Na nano-biocomposites display a largely aggregated clay structure, leading to a lower interface between the nanofillers and the polysaccharide chains (Chivrac et al., 2008b). On the contrary, both the organo-modified sepiolite and montmorillonite display similar effective nanoscale dispersion. Thus, the higher stiffness values recorded for the WS/OSEP-4CS nano-biocomposites are likely due to the strong interactions between starch and sepiolite and the new crystalline structure which increases the crystallinity of the material.

Compared to the neat matrix, a small decrease in the strain at break is obtained with the incorporation of the SEP-Na nanofiller. This decrease is likely due to the global increase in the plasticized starch crystallinity, which is known to reduce the strain at break (Van Soest & Essers, 1997). Regarding the WS/OSEP-1CS samples, a strong decrease in the strain at break value is observed. This decrease is a direct consequence of the large clay aggregates observed by optical microscopy which embrittle the materials. Moreover, a relationship between the amount of cationic starch and the strain at break values is observed, the highest values being obtained for the nano-biocomposites elaborated with the highest cationic starch contents (OSEP-4CS and OSEP-6CS). If we compare the strain at break values of both WS/MMT-Na and WS/OMMT-CS nano-biocomposites, one can see that the WS/MMT-Na display lower values than those of the neat matrix. As for the Young's modulus evolution, this tendency is due to the MMT-Na aggregates, which embrittle the hybrids materials. On the contrary, WS/OMMT-CS nano-biocomposites present a constant strain at break, close to the value of the neat matrix and slightly lower than the WS/OSEP-4CS one. Thus, for both nanofillers organo-modified with cationic starch, the strain at break properties are retained even with this stiffness increase.

Finally, the stress at break properties of both the neat plasticized starch matrix and the nano-biocomposites highly depend on the nanofillers dispersion state and nature. The incorporation of MMT-Na into the plasticized starch matrix induces a decrease in the stress at break value, mainly because of the poor dispersion quality obtained with this nanofiller. On the contrary, WS/OMMT-CS nano-biocomposites display an increase in this value linked to the exfoliated morphology achieved in these materials. Moreover, all sepiolite-based nano-biocomposites present higher stress at break values compared to the neat matrix and the WS/OMMT-CS nano-biocomposites. These raises are linked to the stronger interactions established between the sepiolite nanofillers and the polysaccharide chains and to the new crystalline structure induced by the sepiolite incorporation into the material, both phenomena generating a high stiffness increase.

In conclusion, from a mechanical point of view, these analyses have highlighted the great potential of sepiolite compared to montmorillonite. Indeed, this needle-shaped nanofiller induces significantly higher Young modulus and stress at break values compared to the corresponding montmorillonite nano-biocomposites. This higher reinforcement efficiency of sepiolite compared to montmorillonite has also been observed and reported for PA6 nanocomposites (Bilotti et al., 2009; Xie et al., 2007) and for gelatin nano-biocomposites (Fernandes et al., 2009) and this behavior has been mainly attributed to the numerous silanol groups of sepiolite that allow a good nano-dispersion and very strong interactions with the matrix, resulting in an efficient interfacial stress transfer.

Various studies on nanocomposites materials have intended to compare sepiolite with nanofillers of different type and aspect ratio (Bhattacharya et al., 2009; Fernandes et al., 2009; Garcia et al., 2009; Xie et al., 2007). As previously mentioned, all these studies have highlighted the great reinforcement efficiency of sepiolite which is similar or better than montmorillonite. For styrene butadiene rubber the sepiolite reinforcement efficiency is even presented as similar to carbon nanofibers (Bhattacharya et al., 2009).

Due to its needle-like shape, its size and specific aspect ratio it is indeed very interesting to compare the behavior of sepiolite not only to montmorillonite lamellar clay but also to nanofibers. For that, a survey of the recent literature shows that various studies were dedicated to starch/cellulose whiskers nanocomposites. Tunicin whiskers have been tested as nanofillers in waxy maize starch plasticized by glycerol or sorbitol (Mathew & Dufresne, 2002; Mathew, Thielemans, & Dufresne, 2008; Neus Angles & Dufresne, 2000, 2001). As previously mentioned, glycerol-plasticized starch transcrystallinity at the interface of whiskers surface has been observed but the whiskers also induce a change in phase distribution resulting in the plasticizer to come near the cellulose nanofiller surface. Thus tunicin whiskers do not improve the mechanical properties of glycerol-plasticized starch due to the lack of stress transfer at the matrix/filler interface. Nevertheless, when using sorbitol as plasticizer no change in phase distribution was observed. Thus, the addition of tunicin whiskers, above threshold content, resulted in an improvement of the material stiffness due to a percolating network and to the strong hydrogen interactions between the starch matrix, the sorbitol and the whiskers (Mathew et al., 2008). These trends have also been observed for cassava bagasse cellulose nanofibers reinforcing cassava starch plasticized with glycerol and/or sorbitol (Teixeira et al., 2009).

Interestingly, Dufresne and co-workers (Neus Angles & Dufresne, 2001) have highlighted that the lack of mechanical reinforcement from tunicin whiskers in glycerol-plasticized starch disagree with results obtained with cellulose microfibrils as the starch filler. This behavior has been assigned to the rod-like structure of whiskers and thus the absence of tangling effect of these nanofibers. Such important difference between nanowhiskers and microfibrils has been recently confirmed for PCL-based materials (Siqueira, Bras, & Dufresne, 2009). Finally, cellulose nanowhiskers have been compared to hectorite nanoclay as fillers in sorbitol-plasticized potato starch (Kvien, Sugiyama, Votrubec, & Oksman, 2007). This study have shown that the mechanical properties determined by tensile tests are very similar for the two types of nanofillers, both increasing the starch stiffness while retain elongation at break.

Then, even if comparison are very difficult to make since starch mechanical properties strongly depend on the starch botanical source, the type and content of plasticizers as well as the storage relative humidity, it seems that montmorillonite, cellulose nanowhiskers and sepiolite have rather similar influence on starch mechanical properties.

Interestingly, unlike tunicin nanowhiskers, sepiolite addition increases the stiffness of glycerol-plasticized starch. But, based on other specific properties such as the induced starch transcrystallinity at the filler interface and the related reinforcement efficiency, one can assume that sepiolite needle-shape clay behaves more closely to cellulose rod-like nanowhiskers. Nevertheless, to fully confirm these trends and statements, an additional complete study will have to be carried out on these systems focusing on the nano-biocomposites mechanical properties including fine modeling of their micromechanical behavior.

4. Conclusions

This study reports for the first time on the incorporation of sepiolite, a natural nanofiller presenting a needle-shaped morphology, into plasticized starch matrix. Since previous studies have demonstrated the key role of cationic starch as a montmorillonite compatibilizer to achieve exfoliation into plasticized starch matrices, the first part of this study was dedicated to the elaboration of four different types of organo-modified sepiolite: OSEP-1CS, OSEP-2CS, OSEP-4CS and OSEP-6CS (corresponding to one, two, four and six charge equivalence between the sepiolite and the cationic starch, respectively). Then, nano-biocomposites have been prepared by melt blending technique with the non-modified and the different organo-modified sepiolites.

Morphological analyses have shown that the dispersion of the organo-modified sepiolites led to different micro/nano-structurations depending on the cationic starch content adsorbed on the clay surface. The incorporation of OSEP-1CS into plasticized starch generates large clay aggregates. At higher cationic starch content, this polyelectrolyte fully acts as a compatibilizer and greatly favors the clay dispersion within the plasticized starch matrix, an effective nanoscaled dispersion of the sepiolite needles being obtained. However, this morphology can also be achieved with sodium sepiolite, that is to say without using cationic starch. Besides, it has been pointed out that cationic starch thermal degradation by-products may favor the plasticized starch degradation mechanism and thus reduce the thermal stability of the resulting nanocomposite material.

The added value of sepiolite, has been highlighted by the tensile tests results. All the starch/sepiolite nano-biocomposites displayed a higher Young modulus and stress at break values than the corresponding montmorillonite-based nano-hybrids. Such behavior is linked on one hand to the good affinity between the nanofiller and the polysaccharide chains and on the other hand to the new crystalline structure induced by the sepiolite dispersion which increases the overall material crystallinity. In addition, as already observed for the montmorillonite-based nano-biocomposites, the strain at break properties are retained when the sepiolite needles are well dispersed.

To conclude, this study has clearly highlighted the high potential of the sepiolite nanofillers to enhance the plasticized starch mechanical properties. Indeed, materials properties are even better than those observed for the more classical montmorillonite clay, which already significantly improved the plasticized starch properties. Interestingly, a large survey of the recent literature data seems to indicate that the sepiolite behavior is closer to the natural organic rod-like cellulose nanowhiskers than to the inorganic lamellar nanoclays.

Nevertheless, whereas our previous studies have highlighted the great interest in the use of cationic starch as montmorillonite organo-modifier, the added value of this polycation for the sepiolite organo-modification is less obvious. Indeed, cationic starch content must be high enough to avoid large clay aggregates due to sepiolite flocculation. Moreover, the corresponding materials do not exhibit further improvement in mechanical properties when compared to the nano-biocomposites elaborated with the unmodified sodium sepiolite. In addition, the thermal stability of the corresponding materials is decreased due to the cationic starch degradation by-products. Thus, even if cationic starch does not bring further improvement, sepiolite still appears to be a very powerful option to elaborate plasticized starch materials displaying improved properties.

Acknowledgments

The authors thank the IPCMS-GMI (Institut de Physique et Chimie des Matériaux et du Solide – Groupe des Matériaux Inorganiques) for its technical support. Thanks are also extended to Léon Mentink (Roquette).

References

Alexandre, M., & Dubois, P. (2000). Polymer-layered silicate nanocomposites: Preparation, properties and uses of a new class of materials. *Materials Science & Engineering R – Reports, 28*(1), 1–63.

Averous, L. (2004). Biodegradable multiphase systems based on plasticized starch: A review. *Journal of Macromolecular Science Part C – Polymer Reviews, 44*(3), 231–274.

Averous, L., Fringant, C., & Moro, L. (2001). Plasticized starch–cellulose interactions in polysaccharide composites. *Polymer, 42*, 6565–6572.

Bhattacharya, M., Maiti, M., & Bhowmick, A. K. (2009). Tailoring properties of styrene butadiene rubber nanocomposite by various nanofillers and their dispersion. *Polymer Engineering and Science*. doi:10.1002/pen.21224.

Bilotti, E., Fischer, H. R., & Peijs, T. (2008). Polymer nanocomposites based on needle-like sepiolite clays: Effect of functionalized polymers on the dispersion of nanofiller, crystallinity, and mechanical properties. *Journal of Applied Polymer Science, 107*(2), 1116–1123.

Bilotti, E., Zhang, R., Deng, H., Quero, A., Fischer, H. R., & Peijs, T. (2009). Sepiolite needle-like for PA6 nanocomposites: An alternative to layered silicates? *Composites Science and Technology, 1*, 1–10. doi:10.1016/j.compscitech.2009.07.016.

Bokobza, L., Burr, A., Perrin, M. Y., & Pagnotta, S. (2004). Fibre reinforcement of elastomers: Nanocomposites based on sepiolite and poly(hydroxyethyl acrylate). *Polymer International, 53*(8), 1060–1065.

Bordes, P., Pollet, E., & Averous, L. (2009). Nano-biocomposites: Biodegradable polyester/nanoclay systems. *Progress in Polymer Science, 34*(2), 125–155.

Chen, H., Zheng, M., Sun, H., & Jia, Q. (2007). Characterization and properties of sepiolite/polyurethane nanocomposites. *Materials Science & Engineering, A: Structural Materials: Properties, Microstructure and Processing, 445–446*, 725–730.

Chivrac, F., Gueguen, O., Pollet, E., Ahzi, S., Makradi, A., & Averous, L. (2008a). Micromechanical modeling and characterization of the effective properties in starch based nano-biocomposites. *Acta Biomaterialia, 4*(6), 1707–1714.

Chivrac, F., Pollet, E., & Averous, L. (2009). Shear induced clay organo-modification: Application to plasticized starch nano-biocomposites. *Polymers for Advance Technologies.*. doi:10.1002/pat.1468.

Chivrac, F., Pollet, E., Schmutz, M., & Averous, L. (2008b). New approach to elaborate exfoliated starch-based nanobiocomposites. *Biomacromolecules, 9*(3), 896–900.

Cyras, V. P., Manfredi, L. B., Ton-That, M. T., & Vazquez, A. (2008). Physical and mechanical properties of thermoplastic starch/montmorillonite nanocomposite films. *Carbohydrate Polymers, 73*(1), 55–63.

Darder, M., Lopez-Blanco, M., Aranda, P., Aznar, A. J., Bravo, J., & Ruiz-Hitzky, E. (2006). Microfibrous chitosan – Sepiolite nanocomposites. *Chemistry of Materials, 18*(6), 1602–1610.

Dean, K., Yu, L., & Wu, D. Y. (2007). Preparation and characterization of melt-extruded thermoplastic starch/clay nanocomposites. *Composites Science and Technology, 67*(3–4), 413–421.

Dennis, H. R., Hunter, D. L., Chang, D., Kim, S., White, J. L., Cho, J. W., et al. (2001). Effect of melt processing conditions on the extent of exfoliation in organoclay-based nanocomposites. *Polymer, 42*(23), 9513–9522.

Duquesne, E., Moins, S., Alexandre, M., & Dubois, P. (2007). How can nanohybrids enhance polyester/sepiolite nanocomposite properties? *Macromolecular Chemistry and Physics, 208*(23), 2542–2550.

Fernandes, F. M., Ruiz, A. I., Darder, M., Aranda, P., & Ruiz-Hitzky, E. (2009). Gelatin-clay bio-nanocomposites: Structural and functional properties as advanced materials. *Journal of Nanoscience and Nanotechnology, 9*(1), 221–229.

Garcia, N., Hoyos, M., Guzman, J., & Tiemblo, P. (2009). Comparing the effect of nanofillers as thermal stabilizers in low density polyethylene. *Polymer Degradation and Stability, 94*(1), 39–48.

Kvien, I., Sugiyama, J., Votrubec, M., & Oksman, K. (2007). Characterization of starch based nanocomposites. *Journal of Materials Science, 42*(19), 8163–8171.

Luo, J. J., & Daniel, I. M. (2003). Characterization and modeling of mechanical behavior of polymer/clay nanocomposites. *Composites Science and Technology, 63*(11), 1607–1616.

Ma, J., Bilotti, E., Peijs, T., & Darr, J. A. (2007a). Preparation of polypropylene/sepiolite nanocomposites using supercritical CO_2 assisted mixing. *European Polymer Journal, 43*(12), 4931–4939.

Ma, X., Yu, J., & Wang, N. (2007b). Production of thermoplastic starch/MMT-sorbitol nanocomposites by dual-melt extrusion processing. *Macromolecular Materials and Engineering, 292*(6), 723–728.

Mathew, A. P., & Dufresne, A. (2002). Morphological investigation of nanocomposites from sorbitol plasticized starch and tunicin whiskers. *Biomacromolecules, 3*(3), 609–617.

Mathew, A. P., Thielemans, W., & Dufresne, A. (2008). Mechanical properties of nanocomposites from sorbitol plasticized starch and tunicin whiskers. *Journal of Applied Polymer Science, 109*(6), 4065–4074.

Neus Angles, M., & Dufresne, A. (2000). Plasticized starch/tunicin whiskers nanocomposites. 1. Structural analysis. *Macromolecules, 33*(22), 8344–8353.

Neus Angles, M., & Dufresne, A. (2001). Plasticized starch/tunicin whiskers nanocomposite materials. 2. Mechanical behavior. *Macromolecules, 34*(9), 2921–2931.

Pandey, J. K., & Singh, R. P. (2005). Green nanocomposites from renewable resources: Effect of plasticizer on the structure and material properties of clay-filled starch. *Starch–Starke, 57*(1), 8–15.

Park, H. M., Lee, W. K., Park, C. Y., Cho, W. J., & Ha, C. S. (2003). Environmentally friendly polymer hybrids. Part I. Mechanical, thermal, and barrier properties of thermoplastic starch/clay nanocomposites. *Journal of Materials Science, 38*(5), 909–915.

Park, H. M., Li, X., Jin, C. Z., Park, C. Y., Cho, W. J., & Ha, C. S. (2002). Preparation and properties of biodegradable thermoplastic starch/clay hybrids. *Macromolecular Materials and Engineering, 287*(8), 553–558.

Sinha Ray, S., & Okamoto, M. (2003). Polymer/layered silicate nanocomposites: A review from preparation to processing. *Progress in Polymer Science, 28*(11), 1539–1641.

Siqueira, G., Bras, J., & Dufresne, A. (2009). Cellulose whiskers versus microfibrils: Influence of the nature of the nanoparticle and its surface functionalization on the thermal and mechanical properties of nanocomposites. *Biomacromolecules, 10*(2), 425–432.

Swanson, C. L., Shogren, R. L., Fanta, G. F., & Imam, S. H. (1993). Starch–plastic materials – Preparation, physical properties, and biodegradability (a review of recent USDA research). *Journal of Environmental Polymer Degradation, 1*(2), 155–166.

Teixeira, E. D. M., Pasquini, D., Curvelo, A. A. S., Corradini, E., Belgacem, M. N., & Dufresne, A. (2009). Cassava bagasse cellulose nanofibrils reinforced thermoplastic cassava starch. *Carbohydrate Polymers, 78*(3), 422–431.

Tomka, I. (1991). Thermoplastic starch. *Advances in Experimental Medicine and Biology, 302*, 627–637.

Van Soest, J. J. G., & Essers, P. (1997). Influence of amylose–amylopectin ratio on properties of extruded starch plastic sheets. *Journal of Macromolecular Science, Part A – Pure and Applied Chemistry, 34*(9), 1665–1689.

Van Soest, J. J. G., Hulleman, S. H. D., De Wit, D., & Vliegenthart, J. F. G. (1996). Changes in the mechanical properties of thermoplastic potato starch in relation with changes in B-type crystallinity. *Carbohydrate Polymers, 29*(3), 225–232.

Xie, S., Zhang, S., Wang, F., Yang, M., Séguéla, R., & Lefebvre, J.-M. (2007). Preparation, structure and thermomechanical properties of nylon-6 nanocomposites with lamella-type and fiber-type sepiolite. *Composites Science and Technology, 67*(11–12), 2334–2341.

Zheng, Y. (2006). Study on sepiolite-reinforced polymeric nanocomposites. *Journal of Applied Polymer Science, 99*(5), 2163–2166.